Progress In Electromagnetics Research, PIER 51, 197–217, 2005

MACROSCOPIC PERFORMANCE ANALYSIS OF METAMATERIALS SYNTHESIZED FROM MICROSCOPIC 2-D ISOTROPIC CROSS SPLIT-RING RESONATOR ARRAY

H.-Y. Yao † **and L.-W. Li** ‡

High Performance Computation for Engineered Systems Programme
Singapore-MIT Alliance
Kent Ridge/Cambridge, 119260/02139, Singapore/USA

Q. Wu

Department of Electronics and Communications Engineering
Harbin Institute of Technology
92 Xidazhi Street, Harbin 150001, China

J. A. Kong

Department of Electrical and Computer Engineering
Massachusetts Institute of Technology
Cambridge, MA 02139-4307, USA

Abstract—Two-dimensional isotropic metamaterials fabricated from cross split-ring resonators (CSRRs) are characterized and their constitutive relation tensors are studied in this paper. The effective constitutive parameters of the metamaterials are determined utilizing the quasi-static Lorentz theory and numerical method (i.e., the method of moments for solving the electric field integral equation). The induced current distributions of a single CSRR at the resonant frequency are presented. Moreover, the dependence of the resonant frequency on the dimensions of a single CSRR and the space distances of the CSRR array is also discussed. Reflection and transmission coefficients of a metamaterial slab versus frequency are finally discussed.

† Also with Department of Electrical and Computer Engineering National University of Singapore, Kent Ridge, Singapore 119260

‡ Also with Department of Electrical and Computer Engineering National University of Singapore, Kent Ridge, Singapore 119260 and Department of Electronics and Communications Engineering, Harbin Institute of Technology, 92 Xidazhi Street, Harbin 150001, China

1 Introduction

2 Formulation

3 Effective Constitutive Parameters of a 3-D SRR Array

4 Performances of a Single CSRR and Array

4.1 Effective Permittivity and Permeability

4.2 Currents Distribution of a Single CSRR

4.3 Resonant Frequency

4.4 Reflection and Transmission Coefficients

5 Conclusion

Acknowledgment

References

1. INTRODUCTION

In 1968, Veselago theoretically demonstrated the electromagnetic properties of substances with negative permittivity ε and permeability μ simultaneously [1]. The material is referred to as the left-handed material (LHM) since the electric field $\boldsymbol{E}$, magnetic field $\boldsymbol{H}$ and the wave vector $\boldsymbol{k}$ in the medium obey a left-handed rule. The LHM possesses some unique properties, such as negative refractive index (NRI) and backward-wave propagation (BWP), so that the medium is also often referred to as NRI material. But this kind of media does not exist generally in nature, especially the negative μ of natural materials was not found. Thirty years later, Pendry *et al.* [2–4] relooked into the NRI material, and came up with an idea of perfect lens resulting from the double negative constitutive parameters, ε and μ. The first prediction by Veselago [1] and the later formulation [2–4] of the metamaterials were both theoretical. The research work in this area was not pushed that far, until Smith et al. experimentally realized the LHM for the first time [5]. In his experiment, the composite material consists of two-dimensional periodic arrays of copper split-ring resonators (SRRs) and wires/cylinders. The array of SRRs (of either rectangular or circular shape) is built up for negative magnetic permeability while the wires or cylinders were coupled to the SRRs for negative electric permittivity. The artificial medium has exhibited special properties which can not be observed in the classical media, and it is later referred to as metamaterials.

Thus far, the metamaterials can be fabricated physically by the following common realizations [6]:

- the rectangular and circular split ring resonators [7–9],
- the conducting small particle/object inclusions in dielectric hosting media [10],
- the photonic band gap or photonic crystal structures [11, 12], and
- the L-C microwave striplines or devices [13–15].

The inclusions of metamaterials with the magnetic response can be made from circular SRRs [3], square SRRs [16], and their modified shapes such as the cross SRRs [17]. Other alternatives are distributed L-C network [17, 18] or embedded-circuit transmission line models [19]. In general, most of inclusions make the material properties highly anisotropic. They must be arranged by certain specific ways [3] in order to obtain an isotropic magnetic medium, for example, the three-dimensional magnetic resonator structure CSRR presented by Gay-Balmaz and Martin [17] are highly 2-D isotropy. Several different configurations of CSRRs have been proposed and studied to observe if they are isotropic in terms of the scattering cross section (SCS) [20]. In this paper, we mainly study an array of CSRRs whose geometry is shown in Fig. 1. We aim at analyzing in detail more properties of CSRRs, and they include the material characteristic parameters (permittivity and permeability tensor elements), induced current distributions (using the method of moments) and resonance frequency, because they are quite essential in microwave engineering.

2. FORMULATION

A general form of bianisotropic constitutive relations can be expressed in terms of $\boldsymbol{D}$ and $\boldsymbol{B}$ as a function of $\boldsymbol{E}$ and $\boldsymbol{H}$ [21] as follows:

$$\begin{bmatrix} \boldsymbol{D} \\ \boldsymbol{B} \end{bmatrix} = \begin{bmatrix} \overline{\boldsymbol{\epsilon}} & \overline{\boldsymbol{\xi}} \\ \overline{\boldsymbol{\zeta}} & \overline{\boldsymbol{\mu}} \end{bmatrix} \begin{bmatrix} \boldsymbol{E} \\ \boldsymbol{H} \end{bmatrix}, \tag{1}$$

where $\overline{\boldsymbol{\epsilon}}$ and $\overline{\boldsymbol{\mu}}$ represent the electric permittivity and magnetic permeability tensors, while $\overline{\boldsymbol{\xi}}$ and $\overline{\boldsymbol{\zeta}}$ denote the magnetoelectric cross coupling tensors, respectively.

After taking into account electrically small inclusions, our deductions begin with the electric and magnetic dipole moments $(\boldsymbol{p}_e, \boldsymbol{p}_m)$ based on the quasi-static Lorentz theory [22]. A conducting inclusion with arbitrary shape can be characterized by the generalized electromagnetic polarizability matrix $[\overline{\boldsymbol{\alpha}}]$, which can define the relations between the incident electric and magnetic fields $\boldsymbol{E}^i$ and $\boldsymbol{H}^i$. The induced electric and magnetic dipole moments relate to the

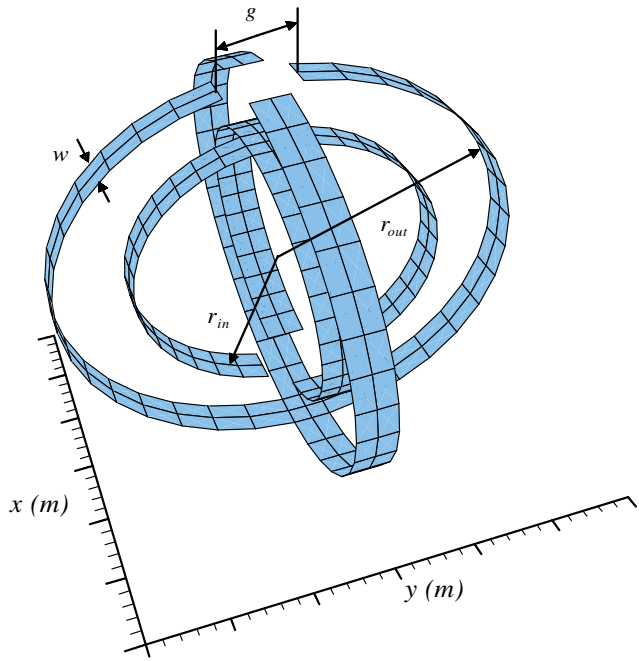

Figure 1. Geometry of a single CSRR where $g = 1\,\text{mm}$, $w = 0.5\,\text{mm}$, $r_{in} = 2\,\text{mm}$, and $r_{out} = 3\,\text{mm}$.

incident electric and magnetic fields as follows:

$$\begin{bmatrix} \boldsymbol{p}_e \\ \boldsymbol{p}_m \end{bmatrix} = \begin{bmatrix} \overline{\boldsymbol{\alpha}}_{ee} & \overline{\boldsymbol{\alpha}}_{em} \\ \overline{\boldsymbol{\alpha}}_{me} & \overline{\boldsymbol{\alpha}}_{mm} \end{bmatrix} = [\overline{\boldsymbol{\alpha}}] \begin{bmatrix} \boldsymbol{E}^i \\ \boldsymbol{H}^i \end{bmatrix}, \tag{2}$$

where

$$\boldsymbol{p}_e = \int_s \rho_e(\boldsymbol{r}) \boldsymbol{r} ds = \frac{i}{\omega} \int_s \boldsymbol{\nabla} \cdot \boldsymbol{J}_e(\boldsymbol{r}) \boldsymbol{r} ds \tag{3a}$$

$$\boldsymbol{p}_m = \frac{\mu_0}{2} \int_s \boldsymbol{r} \times \boldsymbol{J}_e(\boldsymbol{r}) ds \tag{3b}$$

with the electric current $\boldsymbol{J}_e$ on the surface of a conducting inclusion induced by the incident fields.

Using the polarizability matrix $[\overline{\boldsymbol{\alpha}}]$, a general expression for constitutive relations of metamaterials given by Ishimaru *et al.* [23] can be rewritten as

$$\begin{bmatrix} \overline{\boldsymbol{\epsilon}} & \overline{\boldsymbol{\xi}} \\ \overline{\boldsymbol{\zeta}} & \overline{\boldsymbol{\mu}} \end{bmatrix} = \begin{bmatrix} \epsilon_0 \epsilon_h \boldsymbol{U} & 0 \\ 0 & \mu_0 \boldsymbol{U} \end{bmatrix} + \frac{1}{\Delta V} [\overline{\boldsymbol{\alpha}}] \left[\overline{\boldsymbol{U}} - \frac{1}{\Delta V} [\overline{\boldsymbol{C}}] [\overline{\boldsymbol{\alpha}}] \right]^{-1} \tag{4}$$

where ϵ_h is the relative dielectric constant of the host materials, $[U]$ is an unit matrix, while the elementary volume ΔV, the coupling matrix $[\overline{\boldsymbol{C}}]$, and the interaction constant matrix $\boldsymbol{C}$ are defined as

$$\Delta V = d_x d_y d_z, \tag{5a}$$

$$[\overline{\boldsymbol{C}}] = \begin{bmatrix} \boldsymbol{C}/(\epsilon_0\epsilon_h) & 0 \\ 0 & \boldsymbol{C}/\mu_0 \end{bmatrix}, \tag{5b}$$

$$\boldsymbol{C} = \begin{bmatrix} C_x & 0 & 0 \\ 0 & C_y & 0 \\ 0 & 0 & C_z \end{bmatrix}. \tag{5c}$$

The expressions of elements in the matrix C for a three-dimensional array of dipoles can be obtained in terms of the lattice spacings d_x, d_y, and d_z in the corresponding x-, y-, and z-directions [24] as follows

$$C_x = f\left(\frac{d_y}{d_x}, \frac{d_z}{d_x}\right), \tag{6a}$$

$$C_y = f\left(\frac{d_z}{d_y}, \frac{d_x}{d_y}\right), \tag{6b}$$

$$C_z = f\left(\frac{d_x}{d_z}, \frac{d_y}{d_z}\right), \tag{6c}$$

where

$$f\left(\frac{d_y}{d_x}, \frac{d_z}{d_x}\right) = \left(\frac{d_y}{d_x}\right)\left(\frac{d_z}{d_x}\right)\left[\frac{1.202}{\pi} - S\left(\frac{d_y}{d_x}, \frac{d_z}{d_x}\right)\right]. \tag{7}$$

The function $S\left(\frac{d_y}{d_x}, \frac{d_z}{d_x}\right)$ in (7) is defined by:

$$S\left(\frac{d_y}{d_x}, \frac{d_z}{d_x}\right) = \frac{1}{\pi}\sum_{n=-\infty}^{\infty}\sum_{s=-\infty}^{\infty}\sum_{m=1}^{\infty}(2m\pi)^2 K_0\left(2m\pi\left[\left(\frac{nd_y}{d_x}\right)^2 + \left(\frac{sd_z}{d_x}\right)^2\right]^{1/2}\right) \tag{8}$$

while $K_0(\bullet)$ denotes the modified Bessel function of order 0 so that the terms with $n = s = 0$ are excluded. The expressions for $f\left(\frac{d_z}{d_y}, \frac{d_x}{d_y}\right)$ and $f\left(\frac{d_x}{d_z}, \frac{d_y}{d_z}\right)$ have the similar forms.

From Eq. (4), we notice that the polarizability matrix is unknown. To obtain the effective constitutive parameters of the artificial medium, the matrix needs to be evaluated first. According to Eq. (2), the investigation under six different pairs of incident waves $(\boldsymbol{E}^i, \boldsymbol{H}^i)$ is needed. For each pair of incident waves, induced electric currents are

obtained by using the numerical method first, that is, the method of moments. Then the electric and magnetic dipole moments $(\boldsymbol{p}_e, \boldsymbol{p}_m)$ are evaluated using Eqs. (3a) and (3b), and finally six equations can be obtained. Considering all the six pairs of incident waves for all the components of dipole moments, we have theoretically obtained thirty-six scalar equations to determine the thirty-six elements of the polarizability matrix. In the present analysis, we choose (k_x, E_z), $(-k_x, E_z)$, (k_y, E_x), $(-k_y, E_x)$, (k_z, E_y), and $(-k_z, E_y)$ as six incident plane waves.

In the numerical analysis, we omit the thickness of the inclusion and consider it as a thin perfect conductor. In this case, the electric field integral equation (EFIE) is employed. Enforcing the boundary conditions on the surface of the inclusion, the EFIE can be obtained and is given by

$$\widehat{\boldsymbol{t}} \cdot \int_s \left[\boldsymbol{J}_e(\boldsymbol{r}) + \frac{1}{k_0^2} \boldsymbol{\nabla}' \cdot \boldsymbol{J}_e(\boldsymbol{r}') \boldsymbol{\nabla} \right] g(\boldsymbol{r}, \boldsymbol{r}') ds' = -\frac{4\pi i}{k_0 \eta_0} \widehat{\boldsymbol{t}} \cdot \boldsymbol{E}^i(\boldsymbol{r}) \tag{9}$$

where $\widehat{\boldsymbol{t}}$ denotes the unit tangential vector of the inclusion's surface s, η_0 stands for the wave impedance in free space, $g(\boldsymbol{r}, \boldsymbol{r}') = e^{-ik_0|\boldsymbol{r}-\boldsymbol{r}'|}/|\boldsymbol{r}-\boldsymbol{r}'|$ represents the free-space scalar Green's function.

To solve EFIE in Eq. (9), the classical integral equation approach, method of moments (MoM) with curved parametric quadratic surface and roof-top basis functions [25], is used. The surface electric current $\boldsymbol{J}_e$ can be discretized by

$$\boldsymbol{J}_e(\boldsymbol{r}') = \sum_{n=1}^{N} a_n \boldsymbol{j}_n(\boldsymbol{r}'). \tag{10}$$

By applying the method of moments, a linear equation system is yielded and written in a matrix form as follows

$$\overline{\boldsymbol{A}} \cdot \boldsymbol{a} = \boldsymbol{F} \tag{11}$$

in which the elements of the impedance matrix $\overline{\boldsymbol{A}}$ are given by

$$A_{mn} = \int_l dl \boldsymbol{t}_m(\boldsymbol{r}) \cdot \int_{s'} ds' \left[\boldsymbol{j}_n(\boldsymbol{r}') + \frac{1}{k_0^2} \boldsymbol{\nabla}' \cdot \boldsymbol{j}_n(\boldsymbol{r}') \boldsymbol{\nabla} \right] g(\boldsymbol{r}, \boldsymbol{r}') \tag{12}$$

and the elements of $\boldsymbol{F}$ can be evaluated by

$$F_m = -\frac{4\pi i}{k_0 \eta_0} \int_l dl \boldsymbol{t}_m(\boldsymbol{r}) \cdot \boldsymbol{E}^i(\boldsymbol{r}) \tag{13}$$

where $\boldsymbol{t}_m$ represents the testing function, and an denotes the unknown expanding coefficient. Solving Eq. (11) by the conjugate gradient

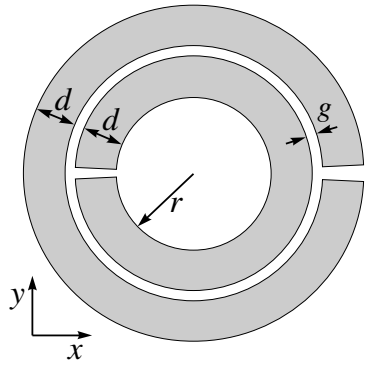

Figure 2. Geometry of a single circular SRR, where $r = 1.5\,\text{mm}$, $d = 0.8\,\text{mm}$, $g = 0.2\,\text{mm}$, and $\Delta V = 8\,\text{mm} \times 8\,\text{mm} \times 3.2\,\text{mm}$.

(CG) method, the unknown surface electric currents are obtained finally. Moreover, the scattered electromagnetic field at any point in the propagation space and the scattering cross section (SCS) can also be evaluated in terms of these currents.

3. EFFECTIVE CONSTITUTIVE PARAMETERS OF A 3-D SRR ARRAY

So far, we can figure out the effective constitutive parameters of a three-dimensional array constructed by conducting inclusions. To demonstrate the efficiency and accuracy of the present approach, we consider a three-dimensional array of split-ring resonators (SRR) shown in Fig. 3. The geometric parameters are taken from [26]. The results of effective constitutive parameters versus the frequency in the rectangular coordinates are shown in Fig. 4. In which, the effective permittivity tensor elements of $\varepsilon_{xx} = \varepsilon_{xxr} - i\varepsilon_{xxi}$, $\varepsilon_{yy} = \varepsilon_{yyr} - i\varepsilon_{yyi}$, and the effective permeability tensor elements of $\mu_{zz} = \mu_{zzr} - i\mu_{zzi}$ are plotted. The other elements are negligibly small according to the numerical results. In these figures, the legends of xx, r and xx, i denote the real and image parts of the element ε_{xx} or μ_{xx}, respectively. The other legends such as yy, r, yy, i, zz, r and zz, i have the similar meanings. It is found that a reasonable agreement is observed by comparing with the data given in [26]. In the MoM computation, the surface of a SRR is discretized into 16 patches and the number N of unknowns is found to be 38 for a well-converged solution. At one frequency point, only 24 conjugate-gradient iterative steps are needed at most for iterative relative error of 10^{-3} to attain the unknowns.

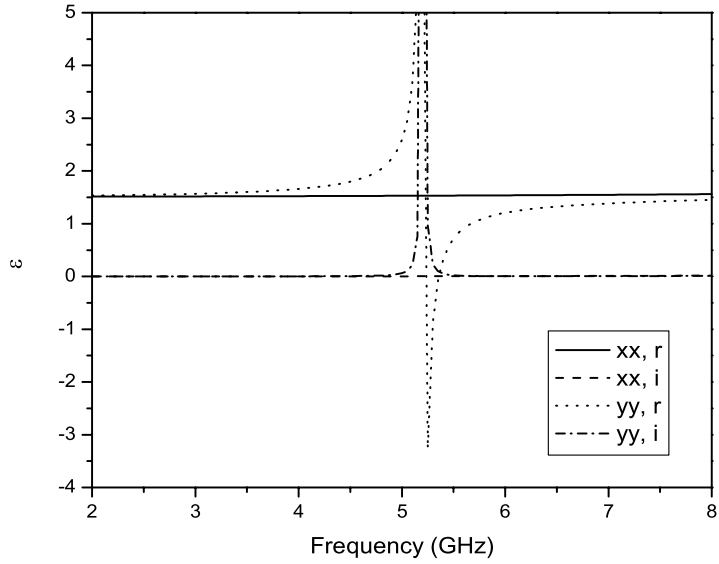

(a) Permittivity

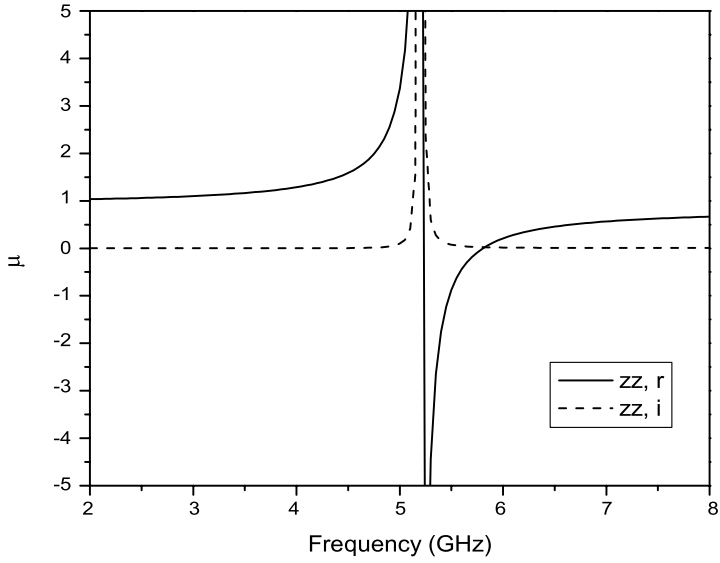

(a) Permeability

Figure 3. Variations of tensor elements ϵ_{xx}, ϵ_{yy}, and μ_{zz} for a 3-dimensional array of circular SRR.

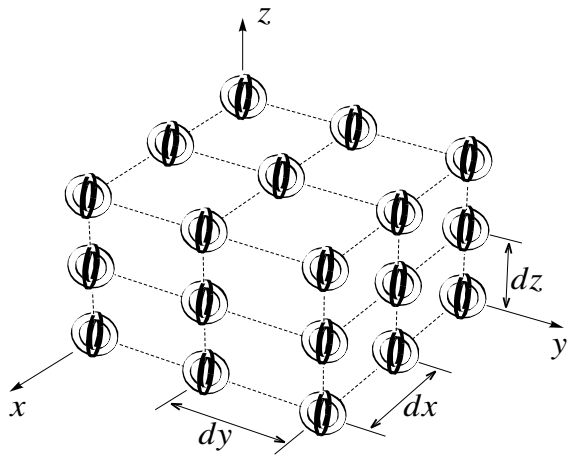

Figure 4. Geometry of a 3-D array synthesized using the CSRRs whose $d_x = d_y = d_z = 8\,\text{mm}$.

Finally, the effective parameters can be obtained very quickly. Due to the versatility of the MoM, we can conveniently evaluate the effective constitutive parameters of a three-dimensional array with arbitrary shaped inclusions. Subsequently, we will analyze an array of CSRRs by using the formulas developed in Section 2.

4. PERFORMANCES OF A SINGLE CSRR AND ARRAY

Geometry of a CSRR under consideration is depicted in Fig. 1. It is composed of two perpendicularly intersecting SRRs. Each SRR is made of two aluminum strips [16]. The structure of CSRR is defined by following parameters: the gap width $g = 1\,\text{mm}$, the strip width $w = 0.5\,\text{mm}$, the inner radius $r_{in} = 2\,\text{mm}$, and the outer radius $r_{out} = 3\,\text{mm}$. A three-dimensional array synthesized using the CSRRs is shown in Fig. 4. The spaces in the corresponding x-, y-, and z-directions are the same and are set as 8 mm.

In order to obtain a magnetic response, we consider the polarization of the incident electric field $\boldsymbol{E}^i$ to be in parallel with the axis of CSRR, that is, the z-axis in the present case. The propagation direction $\boldsymbol{k}_0$ and the polarization of the incident magnetic field $\boldsymbol{H}^i$ are both in the xoy-plane.

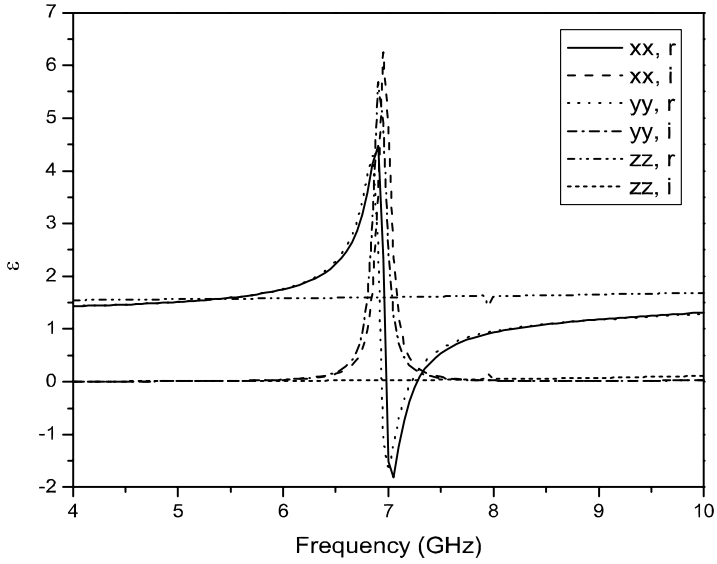

Figure 5. Permittivity tensor elements, ϵ_{xx}, ϵ_{yy} and ϵ_{zz}, versus frequency for a 3-dimensional array of CSRRs.

4.1. Effective Permittivity and Permeability

First of all, we calculate the effective constitutive parameters of the array shown in Fig. 4. In the numerical simulation, a single CSRR is described by 34 parametric quadratic patches and a total of 64 unknowns. We need 40 conjugate gradient iterative steps at most to obtain the converged solution of electric currents. The effective permittivity tensor elements of ε_{xx}, ε_{yy}, and ε_{zz} are shown in Fig. 5 each as a function of frequency. At the same time, Fig. 6 depicts the variations of the effective permeability tensor elements of μ_{xx}, μ_{yy}, and μ_{zz}, respectively. The other off-diagonal elements are negligibly small according to the numerical data, compared with the diagonal elements.

From these figures, we found that the real parts of the permeability and permittivity tensor elements ε_{xx}, ε_{yy}, μ_{xx} and μ_{yy} become negative simultaneously from about 6.9 GHz to 7.3 GHz. Also, the zz-elements, ε_{zz} and μ_{zz}, are almost constant versus frequency. In particular, we can observe that the values of ε_{xx} and ε_{yy} are almost the same, and so are the values of μ_{xx} and μ_{yy}. This clearly demonstrates the 2-dimensional isotropic features of the metamaterial in the xoy-plane. The slight discrepancy is found due to a little coarse step of frequency.

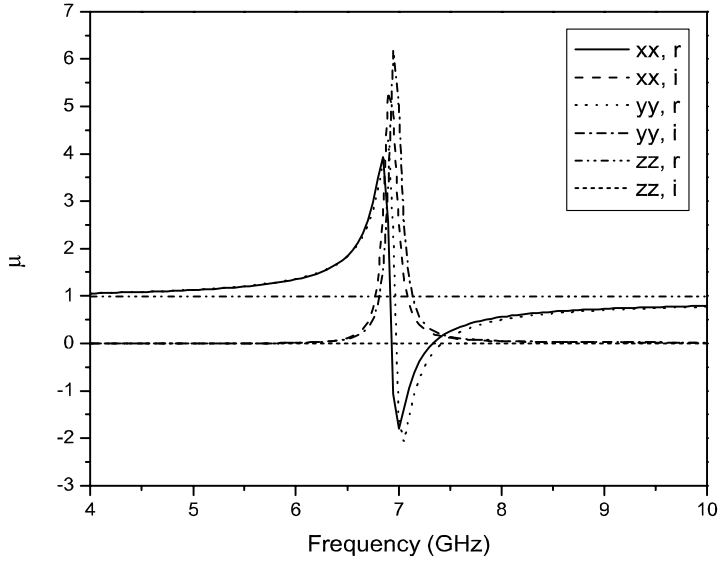

Figure 6. Permeability tensor elements, μ_{xx}, μ_{yy} and μ_{zz}, versus frequency for a 3-dimensional array of CSRRs.

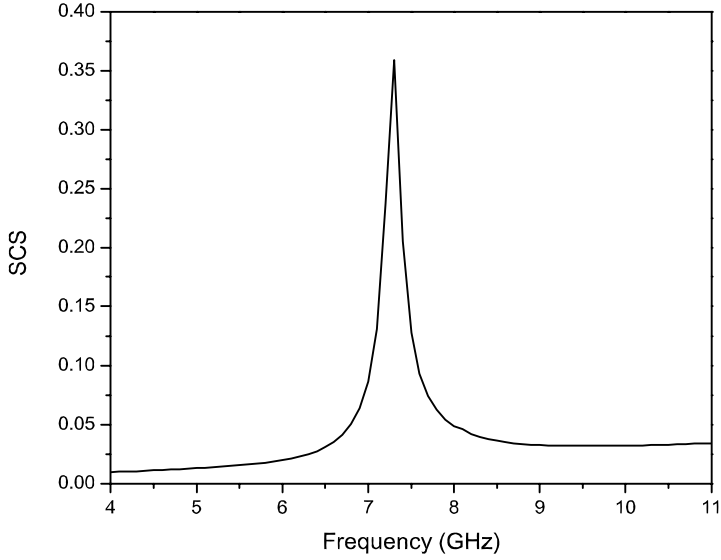

Figure 7. Scattering cross section (SCS) versus frequency for a single CSRR.

4.2. Currents Distribution of a Single CSRR

In this section, we use the SCS to search for the resonant frequency point. For the dimensions of the CSRR shown in Fig. 1, the SCS results are shown in Fig. 7. The resonant frequency is found around 7.3 GHz. To observe the resonance of a single CSRR, we consider the induced current distributions at the resonant frequency. The current distributions of a single inclusion for different incident angles are shown in Fig. 8. When $\phi = 0^\circ$ as shown in Fig. 8(a), the incident magnetic field $\boldsymbol{H}^i$ completely penetrates through the split rings in the yoz-plane, whereas none of $\boldsymbol{H}^i$ through those in the xoz-plane. The induced current densities on their surfaces are much stronger than those in the xoz-plane. The currents vanish at the proximity of the gaps. The strength of the magnetic coupling only depends on the magnetic flux in the SRRs, and therefore we can observe that the current densities on SRRs in the xoz-plane are very weak. For $\phi = 90^\circ$ as shown in Fig. 8(c), the situation is just opposite to that of $\phi = 0^\circ$. For $\phi = 45^\circ$, the result is shown in Fig. 8(b) — this particular angle is such chosen that we can decompose Hi into two components in the xoy-plane, H_x^i and H_y^i, with the same amplitudes. Physically, these figures can help us to better understand wave-material interactions and some resultant phenomena.

For the Fig. 8(b), it is well known that these two magnetic field components penetrate through the split rings in yoz- and xoz-planes, respectively. In consequence, the same current distributions are generated on them. Obviously, the incident magnetic fields can completely penetrate through the cross split-ring resonator, regardless of incident angles. This once again confirms that the CSRR is isotropic in xoy-plane. In these figures, the current densities at the middle of the opposite side to the gaps, which is named by neutral point in [6], become the maximum at the resonant frequency for any incident angle. The charges with opposite sign accumulate on both sides of gaps respectively and thus enhance electrical fields are produced.

4.3. Resonant Frequency

In order to understand the influence of structure dimensions of CSRRs on resonant frequency, we first change the inner radius r_{in} to obtain the different spacing distances t between the inner rings and the outer rings. The resonant frequencies versus different spacing distances t, which range from 0.2 mm to 1.4 mm, are shown in Fig. 9. From this figure, we can find that the resonant frequency increases fast when t becomes larger.

The effects due to other dimensions, such as the gap width g and

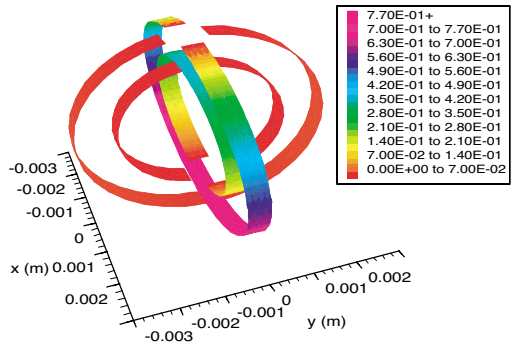

(a) $\phi = 0°$

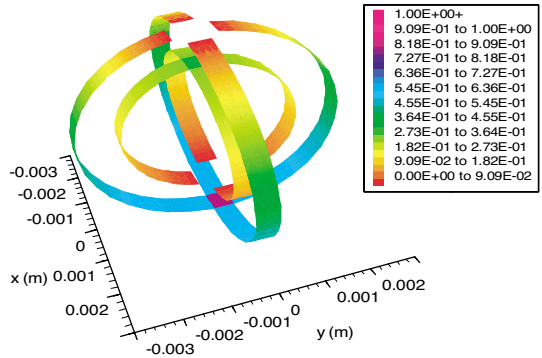

(b) $\phi = 45°$

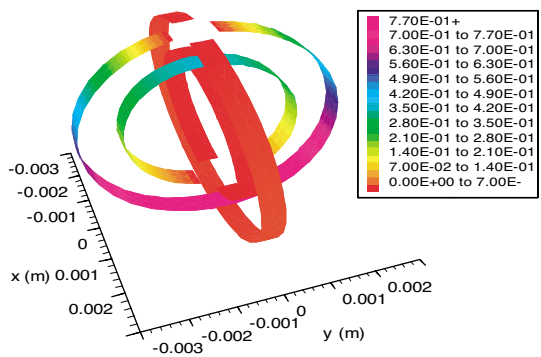

(c) $\phi = 90°$

Figure 8. The induced current density distributions under different incident angles.

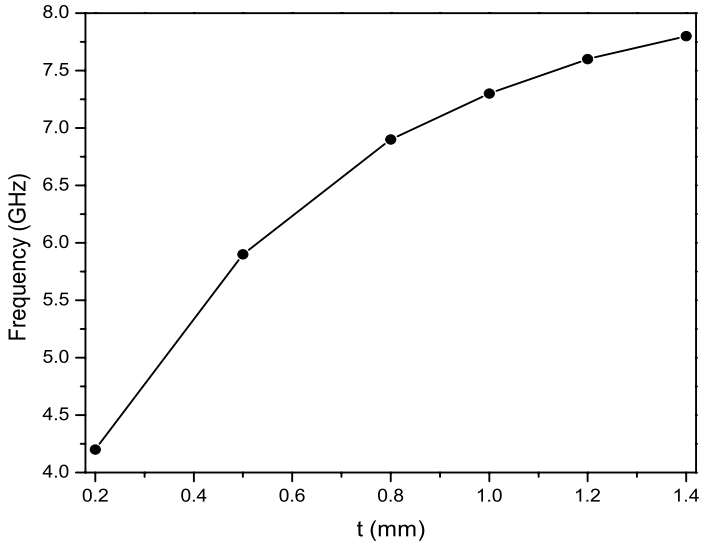

Figure 9. The resonant frequency versus the space distance t.

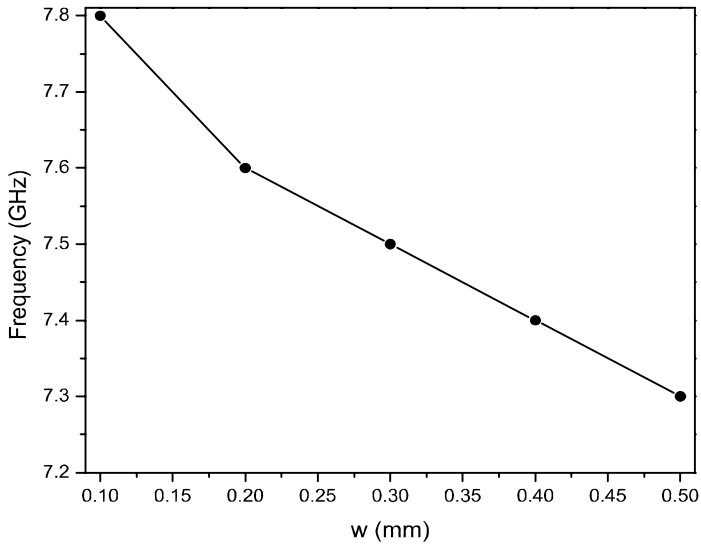

Figure 10. The resonant frequency versus the strip width w.

the strip width w, are also analyzed. We change g from 0.8 mm to 1.4 mm, and w from 0.1 mm to 0.5 mm in the simulation. We find that the change of g affects the resonant frequency slightly. And the narrowing of strip width w can make the resonant frequency increase slowly. We can observe the phenomenon from Fig. 10. These results are consistent with the formulas presented by Pendry *et al.* [3] [referred to Eqs. (42) and (45)]. The capacitance of the gaps affects only slightly the total capacitance and has been omitted in that paper. The increase of t or decrease of w resonant frequency enhanced. Finally, spacing dimensions of the array denoted by d_x, d_y and d_z are considered. We calculate a 3-D array with the number of CSRR in $\widehat{\boldsymbol{x}}$, $\widehat{\boldsymbol{y}}$, and $\widehat{\boldsymbol{z}}$-directions to be 3 and 5, respectively. The space distances are changed from 7 mm to 17 mm with a 2-mm step. We find that the resonant frequency is slightly changed with the increasing of the space distances.

4.4. Reflection and Transmission Coefficients

In this section, an impedance Z is assigned to this discontinuous artificial material, which is considered based on the fact that the wavelength in the material is much larger than the spacing distances and the dimensions of the inclusions. The reflection and transmission coefficients, denoted respectively by r and t, for waves incident normally to the interface between a one-dimensional slab of thickness d and the vacuum are given by [27]

$$r = \frac{Z_2^2 - Z_1^2}{Z_1^2 + Z_2^2 - i2Z_1Z_2/tg\,(k_2 d)} \tag{14a}$$

and

$$t = \frac{1+r}{\sqrt{cos(k_2 d) - iZ_2/Z_1 sin(k_2 d)}} \tag{14b}$$

in which, $k_2 = \omega\sqrt{\varepsilon_2\mu_2}$ is the propagation constant of the incident wave in the artificial material, Z_1 and Z_2 are the impedances of the vacuum and the artificial material, respectively.

Utilizing the foregoing results of effective permittivity and permeability, the variations of reflection and transmission coefficients as a function of frequency f are plotted in Fig. 11, in which the thickness is assumed to be $d = 20$ mm. From Fig. 11, a small passband can be found between about 7.1 GHz and 7.3 GHz, near the resonance of the CSRR.

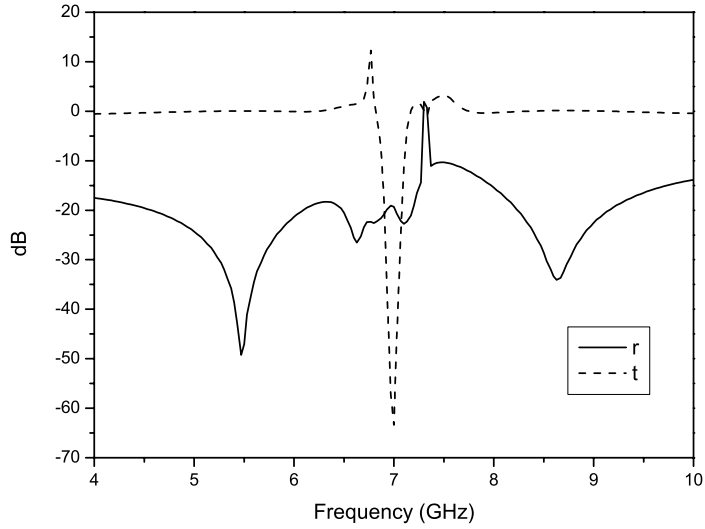

Figure 11. The reflection and transmission coefficients of an artificial material slab.

5. CONCLUSION

Characteristics of an isotropic magnetic resonator and its three-dimensional array are further studied in this paper. To obtain effective constitutive parameters of the artificial medium, elements of polarizability matrix need to be evaluated by a matrix equation, which is constructed by six incident plane waves and the corresponding electric and magnetic dipoles. In this technique, electrical field integral equation (EFIE) is solved using the method of moments (MoM) and then utilized to obtain induced currents on the surface of a cross split-ring resonator (CSRR). This causes us easily analyze a three-dimensional array constructed by arbitrarily shaped inclusions.

From our numerical results, accuracy and applicability of this method are demonstrated. For the three-dimensional array of CSRRs, we can observe a frequency range within which the real parts of four elements, ε_{xx}, ε_{yy}, μ_{xx} and μ_{yy}, appear to have negative values simultaneously. Besides, $\varepsilon_{xx} = \varepsilon_{yy}$ and $\mu_{xx} = \mu_{yy}$ are shown to have the two-dimensional isotropy in material characteristics of this artificial medium. Induced current densities of a single CSRR under different incident angles further verify and physically explain this isotropic property in the xoy-plane. The conclusions drawn in this work agree with those obtained by Martin who utilized this kind of CSRRs to calculate the scattering cross section. Moreover, resonant

frequency resulting from the array structure can be controlled by changing the space distance t between the inner and outer rings, strip width, and/or gap width. Especially, variation of the space distance t can significantly contribute to the resonant frequency. The present results can help us to better understand the physics behind the metamaterials, to gain more insight of the metamaterial's electric characteristics (including the constitutive tensor relations), and to make optimum design in accordance with the practical requirements for fabricating and synthesizing the actual metamaterials for various electromagnetic applications.

ACKNOWLEDGMENT

The authors would like to express their acknowledgment to Singapore-MIT Alliance for its financial support provided during the project where Dr. H. Y. Yao is a Research Fellow and Prof. L. W. Li is a SMA Faculty Fellow.

REFERENCES

1. Veselago, V. G., "The electrodynamics of substances with simultaneously negative values of ε and μ," *Soviet Physics Uspekhi*, Vol. 10, No. 4, 509–514, 1968.
2. Pendry, J. B., A. J. Holden, W. J. Stewart, and I. Youngs, "Extremely low frequency plasmons in metallic meso structures," *Phys. Rev. Lett.*, Vol. 76, 4773–4776, 1996.
3. Pendry, J. B., A. J. Holden, D. J. Robbins, and W. J. Stewart, "Magnetism from conductors and enhanced nonlinear phenomena," *IEEE Trans. Microwave Theory Tech.*, Vol. 47, No. 11, 2075–2084, November 1999.
4. Pendry, J. B., "Negative refraction makes a perfect lens," *Phys. Rev. Lett.*, Vol. 85, No. 18, 3966–3969, October 2000.
5. Smith, D. R., W. J. Padilla, D. C. Vier, S. C. Nemat-Nasser, and S. Schultz, "Composite medium with simultaneously negative permeability and permittivity," *Physical Review Letters*, Vol. 84, No. 18, 4184–4187, May 2000.
6. Li, L.-W., H.-X. Zhang, and Z.-N. Chen, "Representation of constitutive relation tensors of metamaterials: An approximation for ffb media," *Proc. 2003 Progress In Electromagnetics Research (PIERS'03)*, 617, Waikiki Sheraton, Hawaii, USA, October 13–16, 2003.

7. Smith, D. R. and D. Schurig, "Electromagnetic wave propagation in media with indefinite permittivity and permeability tensors," *Physical Review Letters*, Vol. 90, No. 7, 077405, February 2003.
8. Chen, H., L. Ran, J. Huangfu, X. Zhang, K. Chen, T. M. Grzegorczyk, and J. A. Kong, "T-junction waveguide experiment to characterize left-handed properties of metamaterials," *Journal of Applied Physics*, Vol. 94, No. 6, 3712–3716, September 2003.
9. Ziolkowski, R. W., "Design, fabrication, and testing of double negative metamaterials," *IEEE Trans. Antennas Propagation*, Vol. 51, No. 7, 1516–1529, July 2003.
10. Engheta, N., "Metamaterials with negative permittivity and permeability: background, salient features, and new trends," *Microwave Symposium Digest, 2003 IEEE MTT-S International*, Vol. 1, 187–190, 2003.
11. Cubukcu, E., K. Aydin, and E. Ozbay, "Subwavelength resolution in a two-dimensional photonic-crystal-based superlens," *Physical Review Letters*, Vol. 91, No. 20, 207401, November 2003.
12. Shvets, G., "Photonic approach to making a material with a negative index of refraction," *Physical Review B*, Vol. 67, 035109, 2003.
13. Caloz, C., A. Sanada, and T. Itoh, "Microwave applications of transmission-line based negative refractive index structures," *Asia-Pacific Microwave Conference Proceedings*, Seoul, Korea, November 2003.
14. Eleftheriades, G. V., A. K. Iyer, and P. C. Kremer, "Planar negative refractive index media using periodically l-c loaded transmission lines," *IEEE Trans. Microwave Theory and Techniques*, Vol. 50, No. 12, 2702–2712, December 2002.
15. Oliner, A. A., "A planar negative-refractive-index medium without resonant elements," *Microwave Symposium Digest, 2003 IEEE MTT-S International*, Vol. 1, 191–194, 2003.
16. Shelby, R. A., D. R. Smith, S. C. Nemat-Nasser, and S. Schultz, "Microwave transmission through a two-dimensional, isotropic, left-handed metamaterial," *Applied Physics Letters*, Vol. 78, No. 4, 489–491, January 2001.
17. Gay-Balmaz, P. and O. J. F. Martin, "Efficient isotropic magnetic resonators," *Applied Physics Letters*, Vol. 81, No. 5, 939–941, July 2001.
18. Tretyakov, S. A., "Meta-materials with wideband negative permittivity and permeability," *Microwave and Optical Technology Letters*, Vol. 31, 163–165, September 2001.

19. Grbic, A. and G. V. Eleftheriades, "Periodic analysis of a 2-D negative refractive index transmission line structure," *IEEE Trans. Antennas Propagation*, Vol. 51, No. 10, 2604–2611, October 2003.
20. Gay-Balmaz, P. and O. J. F. Martin, "Electromagnetic resonances in individual and coupled split-ring resonators," *Journal of Applied Physics*, Vol. 92, No. 5, 2929–2936, September 2002.
21. Kong, J. A., "Theorems of bianisotropic media," *Proceedings of the IEEE*, Vol. 60, No. 9, 1036–1046, September 1972.
22. Collin, R. E., *Field Theory of Guided Waves*, Chapter 12, IEEE Press, New York, 1991.
23. Ishimaru, A., S.-W. Lee, Y. Kuga, and V. Jandhyala, "Generalized constitutive relations for metamaterials based on the quasi-static lorentz theory," *IEEE Trans. Antennas Propagation*, Vol. 51, No. 10, 2550–2557, October 2003.
24. Collin, R. E., *Field Theory of Guided Waves*, The 2nd edition, IEEE Press, Piscataway, New Jersey, 1991.
25. Song, J. M. and W. C. Chew, "Moment method solutions using parametric geometry," *Journal of Electromagnetic Waves and Applications*, Vol. 9, No. 1/2, 71–83, Jan.–Feb. 1995.
26. Ishimaru, A., S.-W. Lee, Y. Kuga, and V. Jandhyala, "Computation of generalized constitutive relations for metamaterials," *Proceeding of International Symposium on Antennas and Propagation*, Vol. I-02, 177–180, 2002.
27. Kong, J. A., "Electromagnetic wave interaction with stratified negative isotropic media," *Progress in Electromagnetics Research*, PIER 35, 1–52, 2002.

Hai-Ying Yao received the B.Eng. degree in electronic engineering, and M.Eng. degree and Ph.D. degree both in Electromagnetic Field and Microwave Technology all from University of Electronic Science and Technology of China (UESTC), Chengdu, China, in 1996, 1999, and 2002, respectively. From April 2000 to October 2001, she worked at City University of Hong Kong, Hong Kong, SAR China, as a Research Assistant. Since 2002, she has been with High Performance Computations of Engineered Systems (HPCES) Programme of Singapore-MIT Alliance (SMA) as a Research Fellow. Her current research interests include fast algorithms and hybrid methods in computational electromagnetics, and radio wave propagation and scattering in various media.

Le-Wei Li received the degrees of B.Sc. in Physics, M.Eng.Sc. and Ph.D. in Electrical Engineering from Xuzhou Normal University, Xuzhou, China, in 1984, China Research Institute of Radiowave Propagation (CRIRP), Xinxiang, China, in 1987 and Monash University, Melbourne, Australia, in 1992, respectively. In 1992, he worked at La Trobe University (jointly with Monash University), Melbourne, Australia as a Research Fellow. Since 1992, He has been with the Department of Electrical Engineering at the National University of Singapore where he is currently a Professor. Since 1999, he has been also part-timely with High Performance Computation of Engineered Systems (HPCES) Programme of Singapore-MIT Alliance (SMA) as a SMA Fellow. His current research interests include electromagnetic theory, radio wave propagation and scattering in various media, microwave propagation and scattering in tropical environment, and analysis and design of antennas. In these areas, he, as the principal author of a book entitled *Spheroidal Wave Functions in Electromagnetic Theory* by John Wiley in 2001, has published 39 book chapters, over 200 international refereed journal papers, 25 regional refereed journal papers, and over 200 international conference papers. He serves as an Associate Editor of *Journal of Electromagnetic Waves and Applications* and *Radio Science*, an Editorial Board Member of *IEEE Transactions on Microwave Theory and Techniques, Electromagnetics journal*, and an Overseas Editorial Board Member of *Chinese Journal of Radio Science*.

Qun Wu obtained his B.Sc. degree in Radio Engineering, M.Eng. degree in Electromagnetic Fields and Microwave Technology, and Ph.D. degree in Communication and Information Systems Engineering, all at Harbin Institute of Technology (HIT), Harbin, China in 1977, 1988, and 1999, respectively. He worked as a Visiting Professor at Seoul National University (SNU) in Korea, from 1998 to 1999, and Pohang University of Science and Technology, from 1999 to 2000. Since 1990, he has been with Department of Electronic and communication Engineering at HIT, China, where he is currently a Professor. He received two Third-Class Prizes and one Second-Class Prize of Scientific Progress Awards from the Ministry of Aerospace of China in 1989 and 1992, respectively. Dr Wu has published over 30 international and regional refereed journal papers. His recent research interests are mainly in microwave active circuits, electromagnetic compatibility, MMIC, and millimeterwave MEMS devices.

Jin Au Kong is a Professor of Electrical Engineering at the Massachusetts Institute of Technology. His research interest is in the area of electromagnetic wave theory and applications. He has published eight books, including *Electromagnetic Wave Theory* by Wiley Interscience, over 400 referred articles and book chapters, and supervised over 120 theses. He is Editor-in-Chief of the *Journal of Electromagnetic Waves and Applications*, Chief Editor of the book series *Progress in Electromagnetics Research*, and Editor of the Wiley Series in remote sensing.